Photoemission and density functional theory study of Ir(111); energy band gap mapping

2010 J. Phys.: Condens. Matter 22 135006

(http://iopscience.iop.org/0953-8984/22/13/135006)

IOP Publishing Journal of Physics: Condensed Matter

J. Phys.: Condens. Matter **22** (2010) 135006 (6pp) doi:10.1088/0953-8984/22/13/135006

Photoemission and density functional theory study of Ir(111); energy band gap mapping

I Pletikosić[1], M Kralj[1], D Šokčević[2], R Brako[2], P Lazić[3] and P Pervan[1,4]

[1] Institut za fiziku, PO Box-304, HR-10 000 Zagreb, Croatia
[2] Institut 'Ruđer Bošković', PO Box-180, HR-10 000 Zagreb, Croatia
[3] Institut für Festkörperforschung (IFF), Forschungszentrum Jülich, 52425 Jülich, Germany

E-mail: pervan@ifs.hr

Received 12 January 2010
Published 25 February 2010
Online at stacks.iop.org/JPhysCM/22/135006

Abstract

We have performed combined angle-resolved photoemission spectroscopy (ARPES) experiments and density functional theory (DFT) calculations of the electronic structure of the Ir(111) surface, with the focus on the existence of energy band gaps. The investigation was motivated by the experimental results suggesting Ir(111) as an ideal support for the growth of weakly bonded graphene. Therefore, our prime interest was electronic structure around the $\bar{\mathrm{K}}$ symmetry point. In accordance with DFT calculations, ARPES has shown a wide energy band gap with the shape of a parallelogram centred around the $\bar{\mathrm{K}}$ point. Within the gap three surface states were identified; one just below the Fermi level and two spin–orbit split surface states at the bottom of the gap.

(Some figures in this article are in colour only in the electronic version)

1. Introduction

Many metal surfaces exhibit gaps in their projected bulk band structure which represent regions within the surface Brillouin zone (SBZ) forbidden for electron propagation. However, due to symmetry breaking at the surface, single particle electronic states may arise within the projected bulk band gap. These are so called surface states [1]. Irrespective of their nature (e.g. Shockley [2] or Tamm type [3]) these states are highly localized at the surface of a crystal.

The existence of the projected electron gaps has proved to be one of the essential channels for the formation of so called quantum well states (QWS) in supported nanostructures (metallic films, quantum wires, dots); grown on well defined metallic substrates [4–6]. In order to benefit from the possibility to design the electronic properties of the supported nanostructure by tailoring its size and shape (quantum size effect) it is important to ensure that the electrons remain localized within the nanostructure itself, which is achieved if the interface between the surface and the supported nanostructure acts as a potential barrier. The most obvious way in which the supporting surface can act as a barrier is by selecting a material having a total energy gap in the band structure (i.e., over the whole surface Brillouin zone), which is a characteristic of semiconductors and insulators. However, as pointed out above, metals possess k-dependent band gaps. Depending on the direction of propagation, electrons within the supported nanostructure may experience potential barriers at the interface, as electronic states in some parts of the (E, k) phase space in the substrate bulk band structure are not allowed. This property of metallic surfaces has been used to create and study well localized electronic states (quantum well states, QWS) within ultrathin overlayer metallic films [5, 6]. It is therefore of great interest to know the surface electronic structure of the supporting material with respect to that of the nanostructure.

Different aspects of epitaxial growth of graphene on solid surfaces have recently attracted significant attention [7, 8]. From the point of view of electronic structure, SiC, with its broad total energy band gap around the Fermi level,

[4] Author to whom any correspondence should be addressed.

provides a weak interaction with graphene overlayers. Indeed, photoemission measurements indicate that the electronic structure of graphene on SiC is fairly unaffected by the substrate [9]. However, the problem of non-uniform graphene thickness impairs the advantages of this substrate [10]. Use of metal substrate surfaces was considered as an alternative route for the large scale growth of graphene layers. Initial STM measurements of graphene on Ru(0001) showed a high structural quality [8]. Unfortunately, the high density of electron states around the Fermi level for the ruthenium surface has an undesirable effect, a strong hybridization of graphene and Ru states [11]. Similar problems exist in growing graphene on Ni(111) surface [12]. Recent experiments with graphene on Ir(111) show that this substrate surface appears to be superior in terms of graphene structural quality [13] and intact electronic Dirac cones [14]. Having in mind that the fascinating electronic properties of pristine graphene originate from the Dirac cones, i.e. conically dispersing electronic bands crossing at the Fermi level (Dirac point), at the K point of the Brillouin zone, it is obvious that the electronic properties of the iridium surface around the $\bar{\mathrm{K}}$-point are of great importance.

Previous photoemission and spin polarized photoemission experiments on the Ir(111) surface were primarily focused on the electronic structure along the bulk Γ–Λ–L high symmetry direction [15–18] which projects onto the centre of the SBZ. Most of the features observed in the photoemission spectra were explained in terms of direct transitions from iridium bulk states. Furthermore, a surface state was observed at around 0.4 eV below the Fermi level [15]. The spin–orbit splitting of the Λ_2 (Λ_3) and Λ_4 bands in the bulk zone centre was determined to be 0.89 eV [15]. The observed photoemission maxima were found to be in good agreement with a fully relativistic one-step theory of photoemission [18].

In the following we present our combined photoemission and DFT investigation of the electronic structure of the Ir(111) surface, with the focus on the region of the SBZ around the $\bar{\mathrm{K}}$ point.

2. Experimental and calculation details

The experiments were carried out in an ultrahigh vacuum chamber with the base pressure in the range of 10^{-8} Pa. The chamber was equipped with standard surface science equipment including rear-view low electron energy diffraction (LEED). For the photoemission experiments we used a Scienta SES-100 hemispherical analyzer, which simultaneously collects photoelectrons at a range of energies (in this experiment typically set to 5 eV) and angles (around 12°), and a discharge lamp as an excitation source. The instrumental resolution of the analyzer in this experiment was around 25 meV, while the angular resolution was better than 0.2°. He I (21.2 eV) and Ne I (16.85 and 16.67 eV) photons were used for excitation in photoemission spectroscopy experiments. The polar angle was changed by rotation of the sample along the $\bar{\Gamma}$–$\bar{\mathrm{K}}$–$\bar{\mathrm{M}}$ high symmetry direction. The $\bar{\mathrm{K}}$ edge is reached by 21.2 eV (16.85 eV) excitation energy at a polar angle of 45° (55°), respectively. The sample holder allowed cooling and heating of the sample in the temperature range between 50 and 1600 K. All photoemission spectra shown in this work were taken at 70 K substrate temperature. The iridium crystal had a nominal purity of 99.99% and was cut with a precision better than 0.1°.

The *ab initio* calculations were performed in the DFT approach, using the VASP (Vienna *ab initio* simulation package) computer code with the Perdew–Burke–Ernzerhof (PBE) functional and projector augmented wave (PAW) method. Spin–orbit coupling was taken into account in all calculations. We calculated the structure parameters of the system, such as the lattice constant of the iridium bulk and the relaxations of the first few layers of Ir(111), and the Kohn–Sham band structure obtained in the process was used to interpret the ARPES spectra.

We first made calculations for the bulk metal, in order to determine the lattice constant at which the energy per atom is minimum, using the primitive monatomic fcc unit cell. The calculated value of 3.88 Å differs slightly from the experimental value of 3.84 Å of the lattice constant of the fcc unit cell. In subsequent calculations we have used the computed values in order to avoid spurious stresses, in particular in surface calculations. In order to calculate the properties of Ir(111) surfaces we used a slab of 18 layers of atoms in the fcc ABC stacking, while along the surface plane (coordinates x, y) the unit cell consisted of one atom per layer. On top of that we put a region of vacuum of around 25 Å, which is needed as the program assumes periodic boundary conditions in all three spatial directions. The vacuum region had to be sufficiently thick so that the repetition in the z direction does not affect the final result of the calculation, i.e. that the electronic states (in particular those close to the Fermi level) do not tunnel through the vacuum region to the next periodically repeated slab. We used a mesh of 81 k-points in the x–y plane, an energy cutoff of 400 eV, and a pseudothermal smearing of the electron occupation. The top three atomic layers were allowed to relax. The first atomic layer relaxed inwards by 0.03 Å, which is about 1.3% of the interlayer separation, and the second and third layer relaxed outwards by around 0.008 Å and 0.015 Å, respectively. The energy gain was 12 meV per surface atom. Upon relaxation, the work function of Ir(111) surface decreased slightly, from 5.55 to 5.53 eV.

3. Experimental results

Figures 1(a) and (b) show ARPES spectra (photoemission intensity maps) of Ir(111), along the $\bar{\Gamma}$–$\bar{\mathrm{K}}$–$\bar{\mathrm{M}}$ high symmetry line, obtained by Ne I and He I photon excitations. The ARPES spectrum obtained by Ne I shows several bands dispersed around the SBZ centre.

The bands at the zone centre (labelled A–E) are clearly seen in the corresponding energy distribution curve (EDC) shown in figure 2(a). The dominant intensity comes from the band indicated by C, which shows a parabolic-like dispersion. We have determined the binding energies of the bands in the surface zone centre as follows: $E_{\mathrm{A}} = 0.93$ eV, $E_{\mathrm{B}} = 1.35$ eV, $E_{\mathrm{C}} = 2.87$ eV and $E_{\mathrm{D}} = 3.99$ eV. From figure 1(a) we can see that two bands cross the Fermi level at $k_{\parallel} = 0.78$ Å^{-1} and at

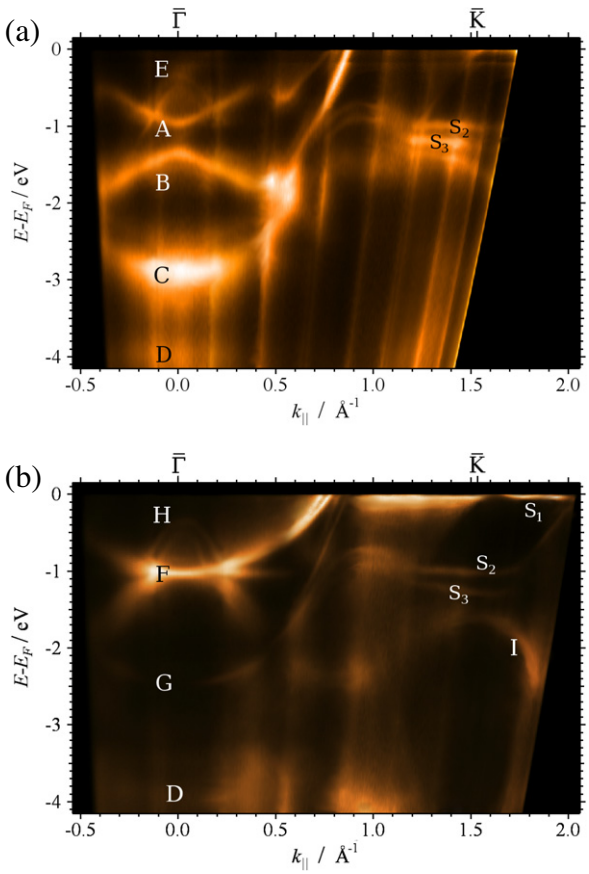

Figure 1. (a) and (b) Photoemission intensity maps as a function of electron binding energy and the component of the electron momentum parallel to the surface along the $\bar{\Gamma}$–$\bar{K}$–$\bar{M}$ high symmetry line, obtained with (a) Ne I and (b) He I excitation.

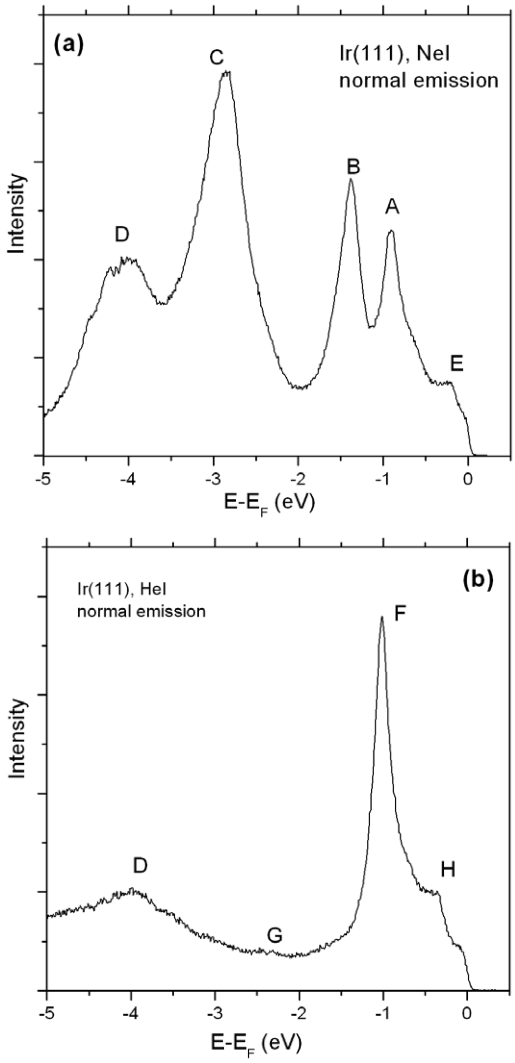

Figure 2. (a) and (b) Normal emission photoelectron energy spectra of graphene on Ir(111) obtained with (a) Ne I, (b) He I excitation.

$k_{||} = 0.86$ Å^{-1}. Close to the zone boundary (around $\bar{K}$ point) one can notice two flat bands (S_2 and S_3) which are somewhat better resolved with 21.2 eV photon energy (figure 1(b)).

The ARPES spectrum obtained by He I shows somewhat less richness in the structure in the SBZ centre. The dominant feature is the band labelled F with its bottom at the surface zone centre 1.04 eV below the Fermi level (F). Figure 2(b) shows the energy distribution curve in the SBZ centre. The band F is dispersed towards the Fermi level and close to it the band bifurcates into two bands crossing the Fermi level at $k_{||} = 0.68$ Å^{-1} and at $k_{||} = 0.72$ Å^{-1}. The band G has a band minimum at 2.4 eV and apparently extends up to the Fermi level with the crossing taking place at $k_{||} = 0.82$ Å^{-1}. However, a closer inspection reveals that the band G disperses only up to $k_{||} = 0.45$ Å^{-1}.

Another distinctive feature of the band structure in the SBZ are two bands (H) that negatively disperse in parallel from the zone centre. However, the corresponding spectra in figures 2(a) and (b), due to the low intensity of the second band, show only a plateau instead of two distinctive peaks.

Finally, we focus our attention to the part of iridium band structure near the Fermi level around the $\bar{K}$ point. This part of the SBZ is characterized by several states showing mainly weak dispersion (S_1, S_2, S_3), clearly visible on both ARPES spectra (figures 1(a) and (b)). However, the He I ARPES map provides a clearer picture of that part of the zone, revealing a wide dark area with shape of parallelogram centred around the $\bar{K}$ point. Across the top edge of the parallelogram there is a noticeably strong photoemission intensity labelled S_1. At the high binding energy side of the parallelogram there are two flat bands (S_2, S_3) dispersing in parallel and a diffused band I exhibiting negative dispersion, with a maximum at around $k_{||} = 1.5$ Å^{-1}. At $k_{||} = 1.68$ Å^{-1} there is an apparently strong change of the dispersion of the state S_2. It almost linearly disperses to lower binding energies, crossing the Fermi level at $k_{||} = 2.2$ Å^{-1}. The dispersion of the S_3 state can not be traced beyond $k_{||} = 1.8$ Å^{-1}. Figure 3 shows energy distribution curves taken from figure 1(b) at several $k_{||}$ points indicated in the figure. All spectra exhibit a pronounced peak at the Fermi level associated with the S_1 band.

4. Band structure calculation

Our calculations of the band structure along the high symmetry directions of the Ir(111) surface Brillouin zone are shown in

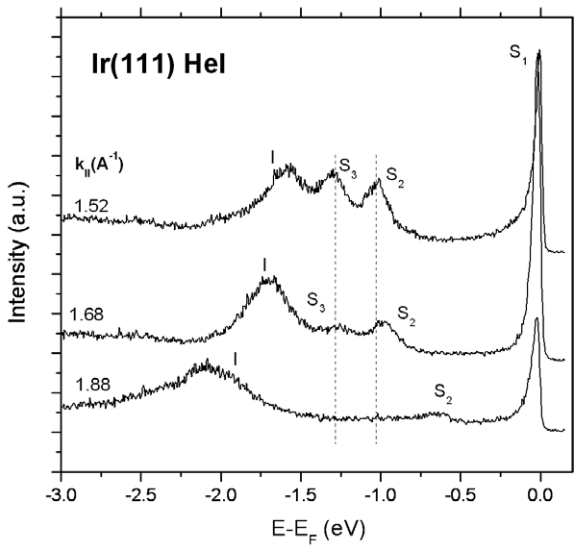

Figure 3. Angle-resolved spectrum from Ir(111) at $k_{\|} = 1.52$ Å^{-1}, i.e. the $\bar{\mathrm{K}}$ point along the $\bar{\Gamma}$–$\bar{\mathrm{K}}$ high symmetry direction.

figure 4. Calculation reveals a number of energy gaps, with clearly defined surface states passing through them. We first analyse the features around the SBZ centre. Near the bottom of the large gap, which extends from 4.45 to 8 eV binding energy, there is a split-off surface state which starts off at 7.63 eV at the zone centre and runs parallel to the bottom of the gap. A similar state exists at around 2.5 eV at $\bar{\Gamma}$, but this one is not situated within the true energy gap but is formed within the low density of bulk bands.

At larger k, between the $\bar{\Gamma}$ and $\bar{\mathrm{K}}$ points of the SBZ several other energy gaps exist. The most interesting is the gap around the $\bar{\mathrm{K}}$ point, starting just below the Fermi level and extending to about 1.6 eV binding energy. Near the bottom of the gap a pair of almost dispersionless states is visible. We have identified them as a spin–orbit split surface state, as the DFT calculation without spin–orbit coupling shows only one state (roughly in between the two shown here). There is another surface state near the top of the gap, just below the Fermi level. Generally it is difficult from this kind of calculation to determine at which values of k a state is a true surface state, and where it becomes a surface resonance by joining a bulk band. However, by comparing the DFT calculation with and without the surface included, we can determine the existence of true surface states in the projected electronic structure.

There is another energy gap between 1.8 and 4 eV binding energy, extending over a large portion of the $\bar{\Gamma}$–$\bar{\mathrm{K}}$ direction. Four spin–orbit split surface states run along the gap. We verified their nature by performing calculations without spin–orbit coupling, as explained above. Further smaller energy gaps are visible at larger binding energies, and virtually all of them support surface states.

5. Discussion

The spectral features in the SBZ centre, shown in figures 1 and 2, exhibit fairly strong dependence on the photon energy, which is in turn a clear signature of the selection rules in the photoemission transitions. The dominant contribution to the photoemission spectra in the zone centre is associated with direct transitions from bulk iridium bands Λ_8^+ and Λ_7^+ [16, 17]. The spectra shown in figures 2(a) and (b) are in full agreement with previous measurements (cf figure 2 in [16]) taking into account the difference in the excitation energies (16.85 eV (this experiment) versus 16 eV in [16]). The 0.85 eV difference in the photon energy does not induce any significant shift of peaks, due to the simple fact that the bands, associated with these spectral maxima, are rather flat or weakly dispersing

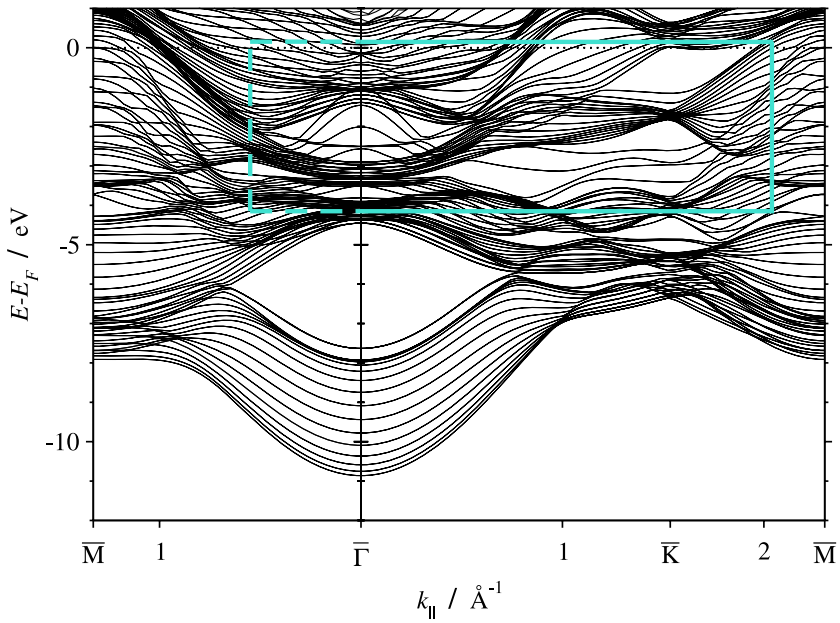

Figure 4. The calculated band structure of Ir(111), along high symmetry directions of the surface Brillouin zone. The light rectangular frame denotes the approximate range of the experimental intensity maps shown in figure 1.

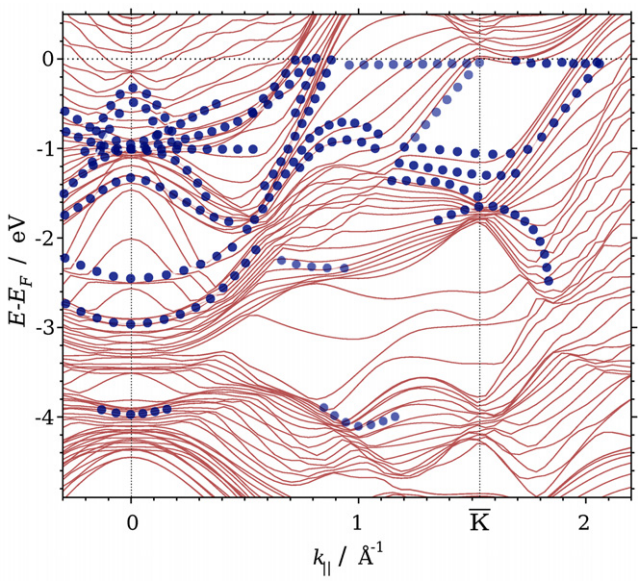

Figure 5. The calculated band structure of Ir(111), along high symmetry directions of the surface Brillouin zone—brown lines (from figure 4) compared to experimental data—dots (taken from figures 1(a) and (b)).

in the part of the surface Brillouin zone where the transition takes place (see e.g. figure 1 in [16]). In contrast to the 16.85 eV excitation energy where several direct transitions of the same strength take place, the spectrum obtained by 21.2 eV is dominated by the maximum at 1.04 eV. The origin of this difference are direct transition rules and is clearly demonstrated in figures 5 and 6 in [18].

Figure 5, which shows combined calculated band structure and experimental data taken from figures 1(a) and (b), generally suggests very good agreement between the calculated band structure and measurements. In the energy range between 1.3 and 3 eV around the SBZ centre, both ARPES maps (figures 1 and 2) indicate the possible existence of an energy band gap, as the corresponding energy range is characterized by very low photoemission intensity. Figure 4 shows that this part of the SBZ is not a true band gap as it is occupied by a low density bulk band. Despite this fact, it looks as if this band structure supports the existence of a surface state. Namely, from figure 5, which summarizes experimental observations with respect to DFT calculations, one can clearly see an s–p-like band which starts off at 2.5 eV at the zone centre and runs parallel to the bottom of the gap. Figure 5 clearly shows that this band should be associated with the band G from figure 1(b). Additional calculations have shown that this band is highly localized at the Ir(111) surface [19], supporting the notion of the surface character of this band. The surface nature of band G also explains our finding that this band disperses up to $k_{\|} = 0.45$ Å^{-1}, where it merges with the bulk states (cf figure 5). Figure 5 also shows good agreement between the energy of band C and the bottom of this energy band gap.

The DFT calculation also shows that the large energy gap extends almost from the zone centre beyond the Brillouin zone edge $\bar{\mathrm{K}}$ within the energy range of 1.8 and 4 eV below the Fermi level. From the comparison of the DFT calculation and the shape of band I (figure 1(b)) we can attribute band I to the top edge of this band gap. However, as figure 5 shows, there is an energy shift (0.3 eV) between the experimental spectrum and the calculated position of the band edge. The origin of this discrepancy is not yet clear. DFT calculations in figure 4 also show that this band gap supports several surface states. While the spectroscopic evidence of this band gap is clear (there are no distinct photoemission features in this portion of the BZ) the same photoemission spectra do not provide any evidence of surface states within the gap. Photoemission spectra in figure 3 do not show maxima which can be associated with these surface states. There might be several reasons for this: symmetry effects or the strong decay of the photo-hole due to the Auger process.

Finally, we turn our attention to the band gap in the shape of a parallelogram centred around the $\bar{\mathrm{K}}$ point. From figures 4 and 5 we see that at the $\bar{\mathrm{K}}$ point two band gaps almost merge and that band I at $k_{\|} = 1.52$ Å^{-1} can also be regarded as the bottom of this parallelogram shaped band gap. In fact, along $k_{\|} = 1.52$ Å^{-1} a large fraction of the SBZ is not occupied by bulk electronic states (see the dotted line in figure 5) and band I is the only bulk band in the wide energy range of 3.8 eV. Based on both the DFT calculation and photoemission spectra we conclude that a large portion of the SBZ around the $\bar{\mathrm{K}}$ point is occupied by a true band gap. The DFT calculation (see figures 4 and 5) suggests that the states depicted in the ARPES maps by S_1, S_2, S_3 are surface states. DFT calculation also shows that S_3 and S_2 bands are spin–orbit split surface states with the spin–orbit splitting somewhat smaller than 0.3 eV (cf figure 3). A large fraction of the S_1 surface band is above the Fermi level (figure 4). The line shape of the S_1 peak in figure 3 supports this conclusion. The other two surface states S_2, S_3 are clearly visible in both ARPES maps (figures 1(a) and (b)). Figure 1(b), obtained by 21.2 eV photon excitation, displays particularly clearly the complete band gap with corresponding surface states. From the figure one can note that surface state S_2 is virtually dispersionless up to $k_{\|} = 1.68$ Å^{-1}, where it apparently changes its direction towards the Fermi level (see also figure 3). The surface state S_3 also shows very weak dispersion with a very strong attenuation of the spectral intensity beyond $k_{\|} = 1.68$ Å^{-1}.

6. Conclusions

We have made a combined theoretical (DFT) and experimental (ARUPS) investigation of the electronic structure of Ir(111) with the focus on the existence on the projected band gaps.

Generally we can conclude that a significant portion of the valence band structure projected to the (111) surface is occupied by bulk band gaps. This notion, based on DFT calculation, is experimentally supported, as we have found a good correspondence between the photoemission maps and the calculated band structure of Ir(111).

Two band gaps extending around the zone centre were identified. The first one appears in the energy range between 1.5 and 3 eV (in the zone centre), which is characterized by the existence of a very small density of the bulk bands.

However, the density of bulk states is small enough for the gap to support a surface state, as predicted by DFT calculation and observed in photoemission spectra. The second band gap extends in the zone centre between 4.5 and 8 eV, with an sp-like surface state dispersing along the bottom of the band. We have spectroscopic evidence of the top of the band gap but not for the surface state.

One of the most prominent features of the projected band structure is the band gap around the $\bar{K}$ point. Three d-like surface states were identified, one at the Fermi level and two spin–orbit split states at around 1 and 1.3 eV below the Fermi level. This band gap has already been proven as essential for the formation of only weakly perturbed graphene on Ir(111).

The large band gap at higher binding energies extends from the $\bar{K}$ point virtually to the zone centre. The photoemission maps provide evidence for the top edge of the gap but not for the surface states as predicted by DFT.

Acknowledgments

Financial support of the Ministry of Science, Education and Sports of the Republic of Croatia through Projects Nos 035-0352828-2840 and 098-0352828-2836 is acknowledged. PL thanks the Alexander von Humboldt foundation for financial support.

References

[1] Bertel E and Donath M (ed) 1994 *Electronic Surface and Interface States on Metallic Systems* (Singapore: World Scientific)
[2] Shockley W 1939 *Phys. Rev.* **56** 317
[3] Tamm I 1932 *Phys. Z. Sov. Union* **1** 733
[4] Smith N V, Brookes N B, Chang Y and Johnson P D 1994 *Phys. Rev.* B **49** 332
[5] Milun M, Pervan P and Woodruff D P 2002 *Rep. Prog. Phys.* **65** 99–142
[6] Pervan P and Milun M 2009 *Surf. Sci.* **603** 1378
[7] Ohta T, Bostwick A, McChesney J L, Seyller T, Horn K and Rotenberg E 2007 *Phys. Rev. Lett.* **98** 206802
[8] Marchini S, Günther S and Wintterlin J 2007 *Phys. Rev.* B **76** 075429
[9] Bostwick A, Ohta T, McChesney J L, Emtsev K V, Seyller T, Horn K and Rotenberg E 2007 *New J. Phys.* **9** 385
[10] Ohta T, El Gabaly F, Bostwick A, McChesney J L, Emtsev K V, Schmid A K, Seyller T, Horn K and Rotenberg E 2009 *New J. Phys.* **10** 023034
[11] Brugger T, Günther S, Wang B, Dil J H, Bocquet M L, Osterwalder J, Wintterlin J and Greber T 2009 *Phys. Rev.* B **79** 045407
[12] Grüneis A and Vyalikh D V 2008 *Phys. Rev.* B **77** 193401
[13] Coraux J, N'Diaye A T, Busse C and Michely T 2008 *Nano Lett.* **8** 565
[14] Pletikosić I, Kralj M, Pervan P, Brako R, Coraux J, N'Diaye A T, Busse C and Michely T 2009 *Phys. Rev. Lett.* **102** 056808
[15] van der Veen J F, Himpsel F J and Eastman D E 1980 *Phys. Rev.* B **22** 4226
[16] Müller N, Kessler B, Schmiedeskamp B, Schönhense G and Heinzmann U 1987 *Solid State Commun.* **61** 187
[17] Tamura E, Piepke W and Feder R 1989 *J. Phys.: Condens. Matter* **1** 6469
[18] Noffke J and Fritsche L 1982 *J. Phys. F: Met. Phys.* **12** 921
[19] Brako R 2008 unpublished